Viscosity and thermal conductivity effects at first-order phase transitions in heavy-ion collisions

D. N. Voskresensky[1, 2, *] and V. V. Skokov[2, **]

[1] *National Research Nuclear University "MEPhI", Russia*

[2] *GSI Helmholtzzentrum für Schwerionenforschung, Darmstadt, Germany*

Effects of viscosity and thermal conductivity on the dynamics of first-order phase transitions are studied. The nuclear gas-liquid and hadron-quark transitions in heavy-ion collisions are considered. We demonstrate that at non-zero thermal conductivity, $\kappa \neq 0$, onset of spinodal instabilities occurs on an isothermal spinodal line, whereas for $\kappa = 0$ istabilities take place at lower temperatures, on an adiabatic spinodal.

1. INTRODUCTION

There are many phenomena, where first-order transitions occur between phases of different densities. In nuclear physics various first-order phase transitions may take place in the Early Universe, in heavy-ion collisions and in neutron stars (e.g., pion condensation, kaon condensation, deconfinement and chiral phase transitions), see reviews [1–3]. At low collision energies the nuclear gas-liquid (NGL) first-order phase transition is possible [1, 5–7]. At high collision energies the hadron-quark gluon plasma (HQGP) first-order transition may occur (see, e.g. [2, 4]). Within a hydrodynamical approach dynamical aspects of the NGL and HQGP transitions were recently studied in [8–12]. An important role of effects of non-ideal hydrodynamics was emphasized. In this talk, we review some results obtained in [8, 9, 11].

2. GENERAL SETUP

Further discussions will be restricted to a description of first-order transition phenomena in the interior region of a dynamical system, e.g. a fireball created in heavy ion collision.

* Electronic address: D.Voskresensky@gsi.de

** Electronic address: V.Skokov@gsi.de

The processes related to the expansion of the fireball to vacuum will not be considered here. Nevertheless, the analysis conducted below will provide a useful insight on a comparison of time needed for a phase transition to occur and the life time of a fireball.

We are interested in a description of long wavelength phenomena at a first-order phase transition. Thereby, we accept an assumption that during a phase transition the velocity of a fluctuation (seed) driving transition, $\mathbf{u}$, is much slower than the mean thermal velocity. Such a description is possible in the framework of the standard system of equations of non-relativistic non-ideal hydrodynamics: the Navier-Stokes equation, the continuity equation, and the equation for the heat transport:

$$mn\left[\partial_t u_i + (\mathbf{u}\nabla)u_i\right] = -\nabla_i P + \nabla_k\left[\eta\left(\nabla_k u_i + \nabla_i u_k - \frac{2}{d}\delta_{ik}\mathrm{div}\,\mathbf{u}\right) + \zeta\delta_{ik}\mathrm{div}\,\mathbf{u}\right], \quad (1)$$

$$\partial_t n + \mathrm{div}(n\mathbf{u}) = 0, \quad (2)$$

$$T\left[\frac{\partial s}{\partial t} + \mathrm{div}(s\mathbf{u})\right] = \mathrm{div}(\kappa\nabla T) + \eta\left(\nabla_k u_i + \nabla_i u_k - \frac{2}{d}\delta_{ik}\mathrm{div}\mathbf{u}\right)^2 + \zeta(\mathrm{div}\mathbf{u})^2, \quad (3)$$

n is the density of the conserving charge (here the baryon density), m is the (baryon) mass, P is the pressure, η and ζ are the shear and bulk viscosities, d is the dimensionality of space, T is the temperature, s is the entropy density, κ is the thermal conductivity.

The simplest (yet non-trivial) example illustrating principal features of a first-order phase transition in a mean-field approximation is the Van der Waals fluid. The adiabatic trajectories, $\tilde{s} \equiv s/n \simeq$ const, for an expansion of a uniform fireball to vacuum, are shown in Fig. 1. The super-cooled vapor (SV) and the overheated liquid (OL) regions are between the Maxwell construction (MC) and the isothermal spinodal (ITS) curves, on the left and on the right respectively. The adiabatic spinodal (AS) curve bounds the AS region from above. For $\tilde{s}_{\rm cr} > \tilde{s} > \tilde{s}_{\rm MC2}$, where $\tilde{s}_{\rm cr}$ corresponds to the value of the specific entropy $\tilde{s}$ at the critical point and the line with $\tilde{s}_{\rm MC2}$ passes through the point $n/n_{\rm cr} = 3$ at $T = 0$, the system traverses the OL state (the region OL in Fig. 1), the ITS region (below the ITS line) and the AS region (below the AS line). For $\tilde{s} > \tilde{s}_{\rm cr}$ the system trajectory passes through the SV state (the region SV in Fig. 1) and the ITS region.

All thermodynamic quantities can be expanded near an arbitrary reference point $(n_{\rm r}, T_{\rm r})$, or $(n_{\rm r}, \tilde{s}_{\rm r})$. Considering the problem in (n, T) variables it is convenient to take the reference point in the vicinity of the critical point $(n_{\rm cr}, T_{\rm cr})$ but outside the fluctuation (critical) region $(n_{\rm cr} \mp \delta n^{\rm fl},\ T_{\rm cr} \mp \delta T^{\rm fl})$ assuming that the latter is very narrow. Note that even in the fluctuation region, a mean-field treatment can be used provided one considers the system at

time scales, being shorter than the scale responsible for a development of long scale critical fluctuations. Thus we further put $(n_{\rm r}, T_{\rm r}) = (n_{\rm cr}, T_{\rm cr})$.

Let us construct a generating functional in the variables $\delta n = n - n_{\rm cr}$, $\delta T = T - T_{\rm cr}$, also called the Landau free energy, such that $\delta(\delta F_L)/\delta(\delta n) = P - P_f + P_{\rm MC}$:

$$\delta F_L = \int \frac{d^3x}{n_{cr}} \left\{ \frac{cm[\nabla(\delta n)]^2}{2} + \frac{\lambda m^3 (\delta n)^4}{4} - \frac{\lambda v^2 m (\delta n)^2}{2} - \epsilon \delta n \right\}, \tag{4}$$

where $\epsilon = P_f - P_{\rm MC}$ is expressed through the pressure at the MC. The maximum of the quantity ϵ is $\epsilon^m = 4\lambda v^3/(3\sqrt{3})$. For the sake of convenience, we will use ϵ normalized to its maximal value, $\gamma_\epsilon = |\epsilon/\epsilon^m|$. The first term in Eq. (4) is due to the surface tension, $\delta F_{L,\,\rm surf} = \sigma S$, S is the surface of the seed. For the Van der Waals equation of state:

$$v^2(T) = -4\frac{\delta T n_{\rm cr}^2 m^2}{T_{\rm cr}}, \quad \lambda_{\rm cr} = \frac{9 f_0}{16}\frac{T_{\rm cr}}{n_{\rm cr}^2 m^3}, \quad \sigma = \sigma_0 \frac{|\delta T|^{3/2}}{T_{\rm cr}^{3/2}}, \quad \sigma_0 = 32 m n_{\rm cr}^2 T_{\rm cr} c. \tag{5}$$

Using Eq. (2), we rewrite Eq. (1) in the dimensionless variables $\delta\rho = v\psi$, $\xi_i = x_i/l$, $i = 1, \cdots, d$, $\tau = t/t_0$ as

$$-\beta\frac{\partial^2\psi}{\partial\tau^2} = \Delta_\xi \left(\Delta_\xi \psi + 2\psi(1-\psi^2) + \widetilde{\epsilon} - \frac{\partial\psi}{\partial\tau} \right), \tag{6}$$

$$l = \left(\frac{2c}{\lambda v^2}\right)^{1/2}, \; t_0 = \frac{2(\widetilde{d}\eta_{\rm r} + \zeta_{\rm r})}{\lambda v^2 \rho_{\rm r}}, \; \widetilde{\epsilon} = \frac{2\epsilon}{\lambda v^3}, \; \beta = \frac{c\rho_{\rm r}^2}{(\widetilde{d}\eta_{\rm r} + \zeta_{\rm r})^2},$$

$\widetilde{d} = 2(d-1)/d$. Only linear terms in the velocity $\mathbf{u}$ were kept in deriving this equation. Since $v^2 \propto -\delta T$, processes in the vicinity of the critical point are proven to be very slow. This is known as the critical slowing down phenomenon.

Eq. (6) should be supplemented by Eq. (3) for the heat transport, which after linearization simplifies to

$$T_{\rm r}\left[\partial_t \delta s - s_{\rm r}(n_{\rm r})^{-1}\partial_t \delta n\right] = \kappa_{\rm r}\Delta\delta T \tag{7}$$

owing to Eq. (2). The variation of the temperature is related to the variation of the entropy density $s[n,T]$ by $\delta T \simeq T_{\rm r}(c_{V,{\rm r}})^{-1}\left(\delta s - (\partial s/\partial n)_{T,{\rm r}}\delta n\right)$, where $c_{V,{\rm r}}$ is the specific heat density.

Note that Eq. (6) differs from the standard Ginzburg-Landau equation exploited in phenomenological approaches. The difference disappears, if one sets the bracketed term in the r.h.s. of Eq. (6) to zero. Superficially this simplification is legitimate, if space-time gradients are small. However, for a seed prepared in a fluctuation at $t = 0$ with a distribution $\delta\rho(t = 0, \mathbf{r})$, the initial condition $\frac{\partial\delta\rho(t,\mathbf{r})}{\partial t}|_{t=0} \simeq 0$ should be fulfilled. Otherwise, because of a positive kinetic energy contribution the probability of fluctuations is suppressed. On

the other hand, the above initial conditions cannot be simultaneously fulfilled, if a differential equation is of a first-order with respect to time derivative. Therefore, there exists an initial stage of the dynamics of seeds ($t \lesssim t_{\rm init}$), which is not described by the standard Ginzburg-Landau equation.

From Eq. (6), it follows, that the time scale for the relaxation of the density is $t_\rho \propto R$, where R is the size of a seed (as we will show below, at some stage overcritical seeds grow with constant velocity), and the time scale for the relaxation of the entropy/temperature, following (7), is

$$t_T = R^2 c_{V,\rm r}/\kappa_{\rm r} \propto R^2. \tag{8}$$

The evolution of a seed is governed by the slowest mode. Thus, for $t_T(R) < t_\rho(R)$, i.e. for $R < R_{\rm fog}$ ($R_{\rm fog}$ is the typical seed size at which $t_\rho = t_T$), dynamics of seeds is controlled by Eq. (6) for the density mode. For seeds with sizes $R > R_{\rm fog}$, $t_T \propto R^2$ exceeds $t_\rho \propto R$ and growth of seeds is slowed down. Thereby, the number of seeds with the size $R \sim R_{\rm fog}$ may increase with time. Estimates [8, 9] show that for the HQGP phase transition $R_{\rm fog} \sim 0.1$–1 fm and for the NGL transition $R_{\rm fog} \sim 1$–10 fm $\lesssim R_{\rm fb}(t_{\rm f.o.})$, where $R_{\rm fb}(t_{\rm f.o.})$ is the fireball size at the freeze-out and $t_{\rm f.o.}$ is the corresponding time. Thus, thermal conductivity effects may manifest themselves in heavy-ion collision dynamics.

Note that seeds of a new phase are produced in an old phase owing to short-scale fluctuations. Fluctuations are not incorporated in the above hydrodynamical equations defined in terms of mean-field variables. Contributions of short-scale fluctuations can be simulated by a random force induced in Eqs. (6), (7), cf. [13].

There are only two dimensionless parameters in Eq. (6), $\widetilde{\epsilon}$ and β. The parameter $\widetilde{\epsilon}$ is responsible for a difference between the Landau free energies of the metastable and stable states. For $t_\rho \gg t_T$ (isothermal stage), $\widetilde{\epsilon} \simeq$ const and dependence on the latter quantity disappears because of $\Delta_\xi \widetilde{\epsilon} \simeq 0$. Therefore, dynamics is controlled only by the parameter β, which characterizes inertia (enters together with the second derivative in time). This parameter is expressed in terms of the surface tension and the viscosity as

$$\beta = (32 T_{\rm cr})^{-1} [\widetilde{d}\eta_{\rm r} + \zeta_{\rm r}]^{-2} \sigma_0^2 m. \tag{9}$$

The larger viscosity and the smaller surface tension, the effectively more viscous (inertial) is the fluidity of seeds. For $\beta \ll 1$ one deals with the regime of effectively viscous fluid

and at $\beta \gg 1$, with the regime of perfect fluid. For the NGL phase transition we estimate $\beta \sim 0.01$. For the HQGP phase transition $\beta \sim 0.02$–0.2, even for the very low value of the ratio $\eta/s \simeq 1/(4\pi)$ [8, 9]. Therefore, the fluidity of density fluctuations in both NGL and HQGP transitions is effectively very viscous.

3. DYNAMICS OF SEEDS IN METASTABLE AREA

Let us consider the stage $t_\rho \gg t_T$. For an expanding system we have to assume that typical time for the formation and evolution of a fluctuation of our interest $t_{\rm form} + t_\rho$ is much smaller than the typical fireball expansion time $t_{\rm f.o.}$. Let us consider the situation, when at very slow expansion with $\tilde{s}(t) \simeq$ const spatially quasi-uniform spherical fireball of a large radius $R_{\rm fb}(t)$ enters either the OL-state or the SV-state (see the corresponding curves in Fig. 1). In case $|n - n_{cr}|/n_{\rm cr} \ll 1$, i.e. in the vicinity of the critical point $(n_{\rm cr}, T_{\rm cr})$, solution (6) describing dynamics of the density in the fluctuation is presented (in the dimensional form) as [8, 9]:

$$\delta n(t,r) \simeq \frac{v(T)}{m}\left[\pm {\rm th}\frac{r - R_n(t)}{l} + \frac{\epsilon}{2\lambda_{\rm cr} v^3(T)}\right] + (\delta n)_{\rm cor}, \tag{10}$$

where the upper sign corresponds to the evolution of bubbles and the lower one to the evolution of droplets, $d = 3$, and the solution is valid for $|\epsilon/(\lambda_{\rm cr} v^3(T))| \ll 1$. The correction $(\delta n)_{\rm cor}$ is responsible for the exact baryon number conservation. Considering r in the vicinity of a bubble/droplet boundary we get equation describing evolution of the seed size:

$$\frac{\beta t_0^2}{2}\frac{d^2 R_n}{dt^2} = \frac{3\epsilon}{2\lambda_{\rm cr} v^3(T)} - \frac{2l}{R_n} - \frac{t_0}{l}\frac{dR_n}{dt}. \tag{11}$$

From this equation, it follows, that a bubble of an overcritical size $R > R_{\rm cr} = 4l\lambda_{\rm cr} v^3(T)/(3\epsilon)$ of the stable gas phase, or respectively a droplet of the liquid phase, been initially prepared in a fluctuation, will grow. On the early stage of the evolution the size of the bubble/droplet $R_n(t) > R_{\rm cr}$ grows with an acceleration. Then, it reaches a steady grow regime with a constant velocity $u_{as} = \frac{3\epsilon l}{\lambda_{\rm cr} v^3(T) t_0} \propto \gamma_\epsilon |T_{\rm cr} - T|^{1/2}$. In the interior of the seed $\delta n \simeq \mp v(T)/m$. The correction $(\delta n)_{\rm cor} \simeq v(T) R_n^3(t)/(m R_{\rm fb}^3)$ is very small for $R_n(t) \ll R_{\rm fb}(t)$.

Substituting Eq. (10) to Eq. (7) for $T =$ const we obtain

$$\delta s = \left(\frac{\partial s}{\partial n}\right)_T \left\{\frac{v(T)}{m}\left[\pm {\rm th}\frac{r - R_n(t)}{l} + \frac{\epsilon}{2\lambda_{\rm cr} v^3(T)}\right] + (\delta n)_{\rm cor}\right\}. \tag{12}$$

While the temperature is constant in the interior and exterior of the seed, the entropy and the density are different in the interior and exterior regions. Nevertheless the approximation

of a quasi-adiabatic expansion of the system might be used even, when the system reaches metastable region, provided the gas of seeds is rare, or $v(T)$ is small.

In Fig. 2 we demonstrate numerical solutions of the hydrodynamical equations in two dimensions ($d = 2$) at the stage $t_\rho \gg t_T$. We take $T/T_{\rm cr} = 0.85$ and compute the configuration for $\eta \simeq 45$ MeV/fm^2 and for $\beta = 0.2$ (effectively large viscosity). The choice $T_{\rm cr} = 162$ MeV, $n/n_{\rm sat} = 1.3$ ($n_{\rm sat} = 0.16$ fm^{-3}) is relevant for the HQGP phase transition. We see that undercritical seeds (disks) dissolve rather rapidly (typical time is $\sim$ several fm) but overcritical seeds grow very slowly. Similar solutions exist for bubbles. Therefore, one can hardly expect to observe a manifestation of large size droplet/bubble remnants in heavy-ion collisions.

The limit $\kappa = 0$ is specific. In case $|n - n_{P,\max}|/n_{P,\max} \ll 1$, i.e. in the vicinity of the point $(n_{P,\max}, \tilde{s}_{P,\max})$, corresponding solutions of Eq. (6) describing dynamics of the density can be presented in the form (10) with the only difference that δT should be replaced by $\delta\tilde{s}$, $\lambda_{\rm cr}$ by $\lambda_{P,\max}$ and $v(T)$ by $v(\tilde{s})$. Dynamics of $R_n(t)$ is determined by Eq. (11), where one should replace values calculated at $(n_{\rm cr}, T_{\rm cr})$ to the corresponding values at $(n_{P,\max}, \tilde{s}_{P,\max})$. From Eq. (6) we obtain $\delta\tilde{s} = 0 = (\delta s n_{P,\max} - s_{P,\max}\delta n)/n^2_{P,\max}$ with δn given by Eq. (10). From known values δs and δn we can define δT. Therefore, not only the density, n, but also the entropy density, s, and the temperature, T, vary in the surface layer and exhibit different values inside and outside a seed. Contrary, the value $\tilde{s}$ remains constant.

4. INSTABILITIES IN SPINODAL REGION

In this section the "r"-reference point can be taken arbitrary, therefore, we suppress the subscript "r". To find solutions of the hydrodynamical equations we put, cf. [8, 9],

$$\delta n = \delta n_0 \exp[\gamma t + i\mathbf{pr}], \quad \delta s = \delta s_0 \exp[\gamma t + i\mathbf{pr}], \quad T = T_> + \delta T_0 \exp[\gamma t + i\mathbf{pr}], \qquad (13)$$

where $T_>$ is the temperature of the uniform matter. From the linearized equations of nonideal hydrodynamics we find the increment, $\gamma(p)$,

$$\gamma^2 = -p^2 \left[u_T^2 + \frac{(\tilde{d}\eta + \zeta)\gamma}{mn} + cp^2 + \frac{u_{\tilde{s}}^2 - u_T^2}{1 + \kappa p^2/(c_V\gamma)} \right], \qquad (14)$$

$u_T^2 = m^{-1}(\partial P/\partial n)_T$ and $u_{\tilde{s}}^2 = m^{-1}(\partial P/\partial n)_{\tilde{s}}$ are speeds of sound at constant temperature and entropy, respectively. Eq. (14) has three solutions. Expanding the solutions for small

momenta (long-wave limit) we find

$$\gamma_{1,2} \;=\; \pm i u_{\tilde{s}} p + \left[\frac{\kappa}{c_V}\left(\frac{u_T^2}{u_{\tilde{s}}^2}-1\right) - \frac{\tilde{d}\eta+\zeta}{mn}\right]\frac{p^2}{2}, \tag{15}$$

$$\gamma_3 \;=\; -\frac{\kappa u_T^2 p^2}{u_{\tilde{s}}^2 c_V}\left[1 - \frac{u_T^2-u_{\tilde{s}}^2}{u_{\tilde{s}}^2 u_T^2}\left(c + \frac{\kappa u_T^4}{u_{\tilde{s}}^2 c_V^2} - \frac{(\tilde{d}\eta+\zeta)\kappa u_T^2}{mnc_V u_{\tilde{s}}^2}\right)p^2\right]. \tag{16}$$

The solutions $\gamma_{1,2}$ correspond to the sound mode in the long wavelength limit, whereas γ_3 describes the thermal transport mode. Below the ITS line (and above the AS line) $u_T^2 < 0$, $u_{\tilde{s}}^2 > 0$, solutions $\gamma_{1,2}$ correspond to an oscillation and damping, whereas γ_3 describes an unstable growing mode. Below the AS line, since there $u_{\tilde{s}}^2 < 0$ and $u_T^2 < 0$, the modes exchange their roles: the sound modes become unstable, while the thermal mode is damped.

For sufficiently high thermal conductivity and not as small p, $\kappa p^2/(c_V|\gamma|) \gg \nu$, $\nu = (u_{\tilde{s}}^2 - u_T^2)/(-u_T^2)$, within the ITS region the most rapidly growing mode ($\gamma \simeq \gamma_m$, and $p \simeq p_m$) is the density mode:

$$\gamma_m = \gamma_m^{(1,2)} = \frac{(-u_T^2)mn_{cr}}{(2\sqrt{\beta}+1)(\tilde{d}\eta+\zeta)}, \quad p_m^2 = \frac{(-u_T^2)\sqrt{\beta}}{(2\sqrt{\beta}+1)c}.$$

Using these expressions we may rewrite the condition of a high thermal conductivity as $\kappa \gg \nu c_V\sqrt{c}$. Typical radius of structures is $R_m \sim 1/p_m$, it decreases with increasing $|\delta T|$.

The amplitudes of the temperature and density are related by

$$\delta T_0 = \delta n_0 \frac{Ts[1 - n(\partial s/\partial n)_T/s]}{c_V n\,[1+\kappa/(\sqrt{c}c_V)]}. \tag{17}$$

Therefore, the assumption of spatial homogeneity of the system fails right after the ITS region is reached. An aerosol (mist) of bubbles and droplets is formed for a typical time $t_{\rm aer} \sim 1/\gamma_m$. For the Van der Waals equation of state we find that $\delta T_0/\delta n_0 > 0$, i.e. the temperature is larger in denser regions. However, the amplitude of the temperature modulation is rather small for $\kappa \gg \nu c_V\sqrt{c}$.

Let us consider the case of zero shear and bulk viscosities and non-zero, but small thermal conductivity. For $-u_T^2 \ll 1$, i.e. slightly below the ITS line, we get

$$\gamma_m = \gamma_m^{(3)} \simeq \frac{\kappa u_T^4}{4cc_V u_{\tilde{s}}^2}, \quad p_m^2 \simeq -u_T^2/(2c)\,. \tag{18}$$

Thus, in both considered cases the instability occurs at the ITS line. For $\kappa \gg \nu c_V\sqrt{c}$ the most rapidly growing mode corresponds to $\gamma_m^{(1,2)}$ and in the opposite limit to $\gamma_m^{(3)}$.

In Fig. 3 we show the time evolution of the density wave amplitudes given by the first Eq. (13), for an undercritical value of p, $p < p_{\rm cr} = \sqrt{2}/l$ (Fig. 3a), and for an overcritical value (Fig. 3b) for the same choice of the parameters $T/T_{cr} = 0.85$, $T_{\rm cr} = 162$ MeV, $n/n_{\rm sat} = 1.3$, as in Fig. 2. The evolution is more rapid compared to the configuration presented in Fig. 2 and the characteristic time scale $t_{\rm ch} \sim 10$ fm is comparable with the fireball expansion time $t_{\rm f.o.}$. Therefore, we may conclude that in heavy-ion collisions during expansion of the fireball the system may linger in QGP phase at $T < T_{\rm cr}$. This means that the equilibrium value of the critical temperature of the phase transition might be significantly higher than the value which may be manifested in growth of fluctuations in experiments with heavy ions. Fluctuations grow more rapidly with decrease of T below $T_{\rm cr}$, $t_{\rm ch} \sim 1.5T_{\rm cr}/|\delta T|$ fm. Far from the critical point rapid grows of fluctuations reminds effect of a warm champagne. There are prospects for observing specific signatures of fluctuations with a typical size, defined by $1/p_m$, in heavy-ion collisions. Fluctuations of this kind might be distinguishable from ordinary statistical fluctuations.

The limit $\kappa = 0$ is again specific. Below the ITS line and above the AS line, the thermal mode γ_3, which drives the system towards equilibrium for a small thermal conductivity, does not exist for $\kappa = 0$. Therefore, the evolution in the spinodal region is entirely governed by adiabatic sound excitations. The increment γ is given by Eq. (14) with u_T replaced by $u_{\tilde{s}}$:

$$\gamma^2 = -p^2 \left[u_{\tilde{s}}^2 + \frac{(\tilde{d}\eta + \zeta)\gamma}{mn} + cp^2 \right]. \tag{19}$$

Therefore, contrary to the case $\kappa \neq 0$, instability appears, when the system trajectory crosses the AS line rather than the ITS line. The value $u_{\tilde{s}}^2 = -\lambda_{P,\max} v^2(\tilde{s}) = 15\delta\tilde{s}T_{P,\max}/(512m)$ for the particular case of the Van der Waals fluid in the vicinity of the point $(n_{P,\max}, T_{P,\max})$ (taken as the reference point). This result holds also in the case of ideal hydrodynamics, where in addition to $\kappa = 0$, the viscosity coefficients (η, ζ) are zero. From Eq. (7), we find

$$\delta s_0 = \delta n_0 s/n, \quad \delta T_0 = \delta n_0 \frac{Ts[1 - n(\partial s/\partial n)_T/s]}{c_V n}. \tag{20}$$

Thereby, the temperature is modulated similar to the entropy density. For the Van der Waals equation of state we find that $\delta T_0/\delta n_0 > 0$. The amplitude of the temperature modulation is larger than in case of $\kappa \neq 0$, see Eq. (17).

Concluding, for any $\kappa \neq 0$ the solutions of Eq. (14) result in the onset of the instability already for $u_T^2 < 0$ (i.e. below the ITS line rather than below the AS line). Since in reality κ

is indeed nonzero, spinodal instabilities start to develop when the trajectory crosses the ITS line rather than the AS, i.e. at significantly higher temperatures. This favors an observation of signals of the spinodal decomposition in the HQGP phase transition in heavy-ion collisions.

We expect that owing to a manifestation of non-trivial fluctuation effects (especially, of the spinodal decomposition at first-order hadron-quark transition) a non-monotonous behavior of different observables as function of collisional energy may be observed. This experimental analysis will be possible at RHIC, FAIR and NICA. Owing to properties of spinodal decomposition a manifestation of specific structures with typical spatial size may serve as a promising signal of the QCD first-order transition.

Acknowledgments. This work was supported in part by the DFG grant WA 431/8-1.

---

1. P. Chomaz, M. Colonna, and J. Randrup, Phys. Rep. **389**, 263 (2004).
2. E. Shuryak, arXiv: 0807.3033 [hep-ph].
3. N. K. Glendenning, Phys. Rep. **342**, 393 (2001).
4. Z. Fodor and S. D. Katz, JHEP **0404**, 050 (2004); Y. Aoki *et al.*, Nature **443**, 675 (2006).
5. G. Röpke, L. Münchow, and H. Schulz, Phys. Lett. B **110**, 21 (1982).
6. H. Schulz, D. N. Voskresensky, and J. Bondorf, Phys. Lett. B **133**, 141 (1983).
7. M. D'Agostino *et al.*, Nucl. Phys. A **749**, 55 (2005); arXiv: nucl-ex/9906004.
8. V. V. Skokov and D. N. Voskresensky, JETP Letters **90**, 245 (2009).
9. V. V. Skokov and D. N. Voskresensky, Nucl. Phys. A **828**, 401 (2009).
10. J. Randrup, Phys. Rev. C **79**, 054911 (2009).
11. V. V. Skokov and D. N. Voskresensky, Nucl. Phys. A **847**, 253 (2010).
12. J. Randrup, Phys. Rev. C **82**, 034902 (2010).
13. A. Z. Patashinsky and B. I. Shumilo, JETP **50**, 712 (1979).

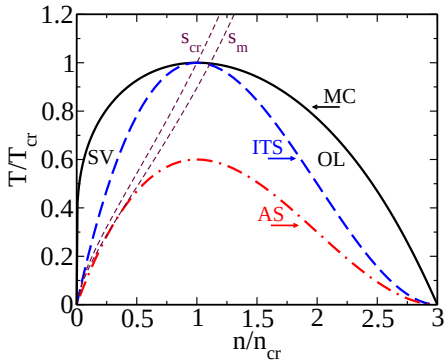

Figure 1. The phase diagram of the Van der Waals equation of state, $T(n)$-plane. The bold solid, dashed and dash-dotted curves demonstrate the boundaries of the Maxwell construction, the spinodal region at $T = \text{const}$ and $\tilde{s} = \text{const}$, respectively. The short dashed lines show adiabatic trajectories of the system evolution: the curve labeled $s_{\rm cr}$ passes through the critical point; s_m, through the maximum pressure point $P(n_{P,\max})$ on the $P(n)$ plane.

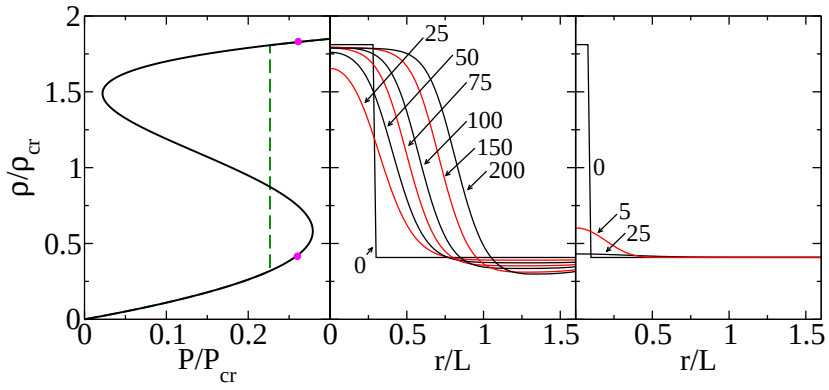

Figure 2. The isotherm for the pressure as a function of the density, with initial and final configurations shown by the dots (left column). The dashed vertical line shows the MC. The initial state represents the stable liquid phase disk ($d = 2$) in metastable SV. Middle column demonstrates the time evolution of the density of the overcritical liquid disk. The numbers near the curves (in L) denote time moments; $r = \sqrt{x^2 + y^2}$, $|\delta T/T_{\rm cr}| = 0.15$, $L = 5$ fm. Right column, the same for the undercritical liquid disk.

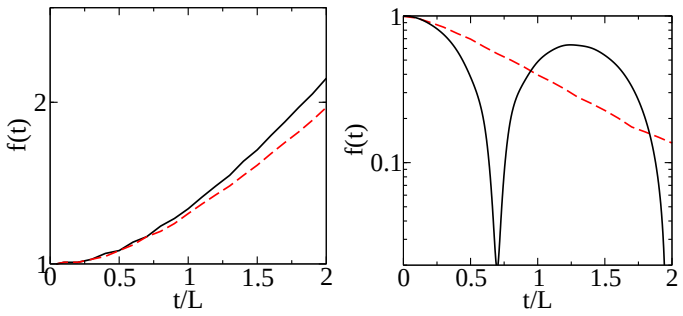

Figure 3. Time evolution of the wave amplitudes $f(t)$ defined as $\delta n(t)$ normalized to the amplitude of the initial disturbance. Solid line is for effectively small viscosity ($\beta = 10$) and dash line, for the large viscosity ($\beta = 0.1$). *a*): the undercritical wave number $p = 2/L$ (growing modes). *b*): the overcritical value $p = 8/L$ (oscillation modes for large β and damped modes for small β). Other parameters are taken to be the same, as in Fig. 2.

FIGURE CAPTIONS

Fig. 1 The phase diagram of the Van der Waals equation of state, $T(n)$-plane. The bold solid, dashed and dash-dotted curves demonstrate the boundaries of the Maxwell construction, the spinodal region at $T = \text{const}$ and $\tilde{s} = \text{const}$, respectively. The short dashed lines show adiabatic trajectories of the system evolution: the curve labeled $s_{\rm cr}$ passes through the critical point; s_m, through the maximum pressure point $P(n_{P,\max})$ on the $P(n)$ plane.

Fig. 2 The isotherm for the pressure as a function of the density, with initial and final configurations shown by the dots (left column). The dashed vertical line shows the MC. The initial state represents the stable liquid phase disk ($d = 2$) in metastable SV. Middle column demonstrates the time evolution of the density of the overcritical liquid disk. The numbers near the curves (in L) denote time moments; $r = \sqrt{x^2 + y^2}$, $|\delta T/T_{\rm cr}| = 0.15$, $L = 5$ fm. Right column, the same for the undercritical liquid disk.

Fig. 3 Time evolution of the wave amplitudes $f(t)$ defined as $\delta n(t)$ normalized to the amplitude of the initial disturbance. Solid line is for effectively small viscosity ($\beta = 10$) and dash line, for the large viscosity ($\beta = 0.1$). *a*): the undercritical wave number $p = 2/L$ (growing modes). *b*): the overcritical value $p = 8/L$ (oscillation modes for large β and damped modes for small β). Other parameters are taken to be the same, as in Fig. 2.